

LINEAR WEIGHT OPTIMIZATION OF LOCAL MAGNETIC FIELD SENSORS FOR THE INTEGRAL FIELD MEASUREMENT IN ACCELERATOR MAGNETS

M. Taupadel*, A. Bellelli, V. Di Capua, A. Lu, C. Petrone, M. Buzio,
V. Kain, S. Russenschuck, CERN, Geneva, Switzerland

Abstract

The measurement of the integral magnetic field in particle accelerator magnets is crucial for their precise control and operation. Traditional methods often rely on a fixed, long integral induction coil, which, however, may be difficult or impossible to install in the magnet bore. This study presents an approach to obtain integral magnetic field measurements through a linear combination of small, local magnetic field sensors. Our methodology involves strategically placing sensors along the magnet to minimize the error between the measured and inferred integral magnetic field. We employ optimization algorithms to determine the optimal number, position, and linear combination weights of sensor readings that best approximate the integral field. We validate our approach through simulation and experimental setups. The results indicate that our optimized sensor placement and weighting scheme can be effectively implemented in existing accelerator systems, offering a scalable solution to support particle accelerator operation.

INTRODUCTION

Particle accelerators depend on the precise control of magnetic fields to guide and stabilize charged particles along their designated trajectories [1]. This is usually achieved by means of magnetic field measurements, either to provide real-time feedback to the RF and other accelerator subsystems, or to enable the development of suitable mathematical models [2]. The required level of accuracy generally falls within the range of 10^{-4} of the peak field [3].

Traditional measurement methods for fast-cycled iron-dominated magnets, typically up to a few hundred Hz of passband, frequently utilize integral induction coils inserted in the bore to capture the full extension of the field, including the fringe regions that extend beyond both ends of the yoke [4]. The manufacture of induction coils up to several meters long is, in itself, a technically challenging task, especially when it comes to achieving precise geometrical tolerances and electrical properties. Accurate calibration of the coil's geometrical parameters, including primarily its effective width [4, 5], requires specialized procedures and dedicated facilities, such as large-size reference dipole magnets or additional instrumentation (e.g. stretched-wire systems). Induction coils, due to their excellent dynamic linearity up to frequencies typically well above this range, are ideally suited to dynamic measurements; however, integration of the induced voltage across these coils is prone to

drift effects, which can significantly affect measurement results [6]. Moreover, the measurement is intrinsically blind to the initial field level, which must be controlled or measured separately. These drawbacks often lead to the incorporation of additional sensors. For example, real-time measurement systems of the bending dipole field, which is the main use case, typically combine the induction coil with a local field sensor, such as nuclear magnetic resonance (NMR) or Hall probe, to provide the approximate integration constant [7, 8]. This kind of setup, known as "B-train", is widely used in research accelerators [7] as well as in hadron therapy centers [8], where achieving the highest possible accuracy is paramount.

The difficulties listed above are compounded by the need to optimize the placement of the magnetic field sensors. The ideal placement is on the magnet axis, as close as possible to the nominal beam path, which is not compatible with operation. An acceptable approximation can be obtained by placing the sensors between the vacuum chamber and the magnet poles. However, such a tight integration must already be foreseen at the early design stage [9]. As an alternative, sensors can be installed in the accessible gap of an additional reference magnet, which should be powered in series with the ring [7]. This solution provides maximum freedom to install and maintain the sensors, however, adding considerably to the complexity and cost of the measurement system [7].

To address these shortcomings, this paper presents an innovative methodology aimed at replacing integral coils with multiple local, point-like magnetic field sensors, focusing on Hall probes as a case study. Using optimization algorithms, we determine the optimal weighting of the sensor readings in order to approximate the integral magnetic field as closely as possible. Due to the small size of the sensors, this approach overcomes most of the limitations listed above by offering a flexible and accurate solution, suitable for arbitrary magnet geometries and power cycles.

PROPOSED METHOD

This paper proposes a method based on local point-like magnetic field sensors to reconstruct the integral field of a dipole. The integral magnetic field is defined by [7] as:

$$\mathbb{I}(t) = \int_{-\infty}^{+\infty} B(t, s) ds, \quad (1)$$

where B represents the relevant field component, s is the longitudinal coordinate along the nominal beam path, and the integration limits are extended to infinity to cover the totality

* maurus.taupadel@cern.ch

of the field generated, assuming an isolated magnet. The integral field can be expressed as a linear combination of k field measurements taken at different longitudinal positions:

$$\hat{\mathbb{I}}(t) = \sum_{i=1}^k w_i \hat{B}_i(t), \quad (2)$$

where $\hat{\mathbb{I}}(t)$ is the reconstructed field integral in Tm, w_i is each sensor's weight in m, and $\hat{B}_i(t)$ represents each sensor's reading in T.

For a given number and position of sensors, the weights are optimized by minimizing with the least-squares method the root mean square error *RMSE*:

$$\min_w RMSE^2, RMSE = \left\| \sum_{i=1}^k w_i \hat{B}_i(t) - \mathbb{I}_{ref}(t) \right\|, \quad (3)$$

where $\mathbb{I}_{ref}(t)$ represents the integral magnetic field obtained with a reference instrument, such as an integral coil. The weights can additionally be set to satisfy the following constraints, transforming (2) into a convex combination [10]:

$$\sum_{i=1}^k w_i = 1, \quad w_i \geq 0 \quad \forall i \in \{1, \dots, k\}. \quad (4)$$

To find the optimal number and position of sensors, we consider initially a set of n possible positions, such as those shown in Fig. 1. The algorithm runs through all possible combinations $N = \binom{n}{k}$ of k sensor positions, which are ranked by their *RMSE*.

The number of sensors k is chosen in a way to balance measurement quality, technical constraints, and cost. Increasing k can be expected to improve field reconstruction by capturing the field behavior in different regions (e.g. the saturated ends), as well as to reduce random noise proportionally to $k^{-1/2}$, although with diminishing returns [11]. Additionally, some redundancy is desirable to enhance system robustness against sensor failure.

EXPERIMENTAL VALIDATION

For the validation of this method, we utilized a spare dipole magnet (MBB type) from the SPS CERN accelerator machine, measured on a dedicated test bench. Whenever a spare magnet is available, this solution allows complete freedom to place sensors leading to a comprehensive characterization, which can be applied with very good approximation to all magnets of the same type.

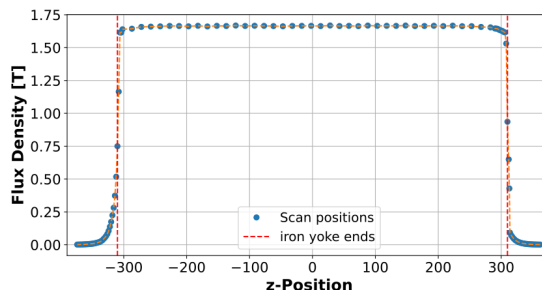
Experimental Setup

The reference field integral was measured with a 7 m induction coil that covers the length of the iron yoke, plus the whole fringe field region to see the complete longitudinal integral of the magnetic field [12]. The coil was calibrated in-situ by means of the single-stretched wire (SSW) method, measuring the absolute integral field including the remanent field contribution as described in [13].

Local magnetic field measurements were performed using a single Analog Hall effect sensor (HE244), which was cross-calibrated against an NMR system across its full operating range to improve measurement precision. To correct for inherent non-linearity, a third-degree polynomial function was applied to the sensor response.



(a) Top view of the SPS dipole magnet. Blue dots indicate scan positions along the longitudinal z -axis.



(b) Magnetic flux density at $n = 114$ positions along the z -axis.

Figure 1: Scan positions and corresponding magnetic flux density distribution along the SPS dipole magnet.

The Hall sensor was moved at 114 different positions as shown in Fig. 1, with a spatial resolution of 15 cm in the central uniform field region. Additionally, a finer resolution of 2 cm was applied to the steep roll-off region at the end of the magnet yoke, which is of special interest due to the gradient decreasing with saturation. The magnet excitation current was pulsed at each position following the same cycle to ensure reproducibility. The current had a ramp rate of 5000 A/s and maintained a flat-top of 4500 A for a duration of 3 s. Changes in the magnet excitation current induce shielding eddy currents in the iron yoke, which delay the magnetic field within the magnet bore. The delay is affected by various design factors, including the properties and dimensions of the iron lamination and the shape and characteristics of the magnet end plates. At each position, the measurement was averaged between $t = 1.8$ s and $t = 3.8$ s, after the eddy currents decayed.

Experimental Results

The results of the optimization algorithm are summarized in Fig. 2, where the RMSE of all combinations tested is plotted for $k = 1$ to 5. We see that configurations based on a number of sensors $k = 4$ represent a good compromise between performance and cost, due to the negligible improvement obtained with 5 sensors.

The best placement found yields an RMSE of about $2 \cdot 10^{-3}$ Tm and is shown in Fig. 3. Three sensors are positioned inside the magnet and one at its edge, where the effects of eddy currents in the end plates are more pronounced. To ensure coverage of these position-dependent

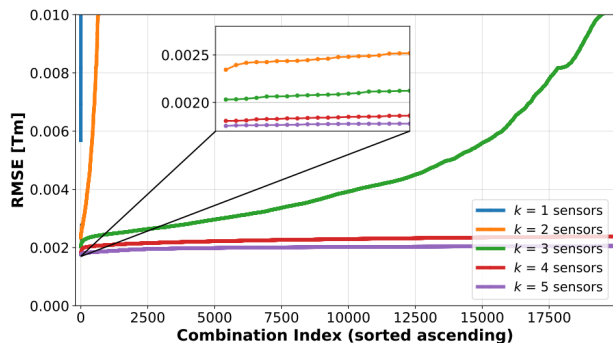


Figure 2: Optimized combinations sorted for lowest RMSE [Tm] with different numbers of sensors.

effects, it is important to place sensors at least in one of the end regions, which should in principle be symmetric.

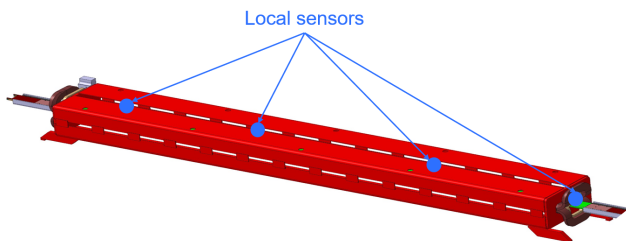


Figure 3: Sensor positions in final configuration.

Low-pass filtering techniques further improve the signal's precision as illustrated in the upper plot of Fig. 4, which shows the integral field signal obtained from the Hall sensor combination and the reference signal. The performance of the filtered Hall sensors compared to the reference can be seen in the lower plot of Fig. 4.

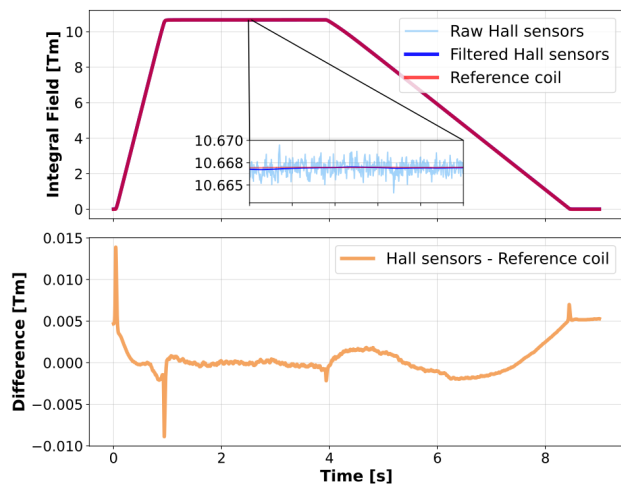


Figure 4: Comparison of the integral field $\hat{I}(t)$ (lightblue) and the low-pass filtered signal $\tilde{I}(t)$ (blue) with the reference integral field $I_{ref}(t)$ (red) with zoom on the flat-top. The lower plot shows the difference between $I_{ref}(t)$ and $\tilde{I}(t)$.

The standard deviation from a single Hall sensor on a field plateau of up to 2 T typically is in the order of $3 \cdot 10^{-4}$ T. Table 1 shows the standard deviation of the combined Hall sensors and the integral coil which, expressed in terms of equivalent average field, is for both at the level of about 10^{-5} T, and is therefore in line with the typical performances of B-Train systems.

Table 1: Standard Deviation (σ) of the Signals between $t = 1.8$ s and $t = 3.8$ s for both Integral Field [Tm] and the equivalent Average Field [T]

Signal	σ_I [Tm]	σ_B [T]
Raw (Hall sensors)	$7.7 \cdot 10^{-4}$	$1.2 \cdot 10^{-4}$
Filtered (Hall sensors)	$8.8 \cdot 10^{-5}$	$1.4 \cdot 10^{-5}$
Reference (integral coil)	$7.8 \cdot 10^{-5}$	$1.2 \cdot 10^{-5}$

Scalability and Practical Implications

The proposed system is inherently scalable and adaptable to various accelerator configurations. Its modular design allows for easy replacement of failed sensors. In case immediate replacement is not possible, redundant sensors can still provide accurate measurements after recalculation of their optimal weights, adapted to the remaining positions. Notably, this intrinsic fault tolerance is achieved with little additional cost, as the integration of supplementary sensors entails minimal financial and infrastructural overhead relative to the overall system. The compact Hall sensors can be installed in tight spaces, such as between the vacuum chamber and the magnet yoke, making them a practical alternative in environments where integral coils are unsuitable.

CONCLUSION

This study introduces a new method for measuring integral magnetic fields. It optimizes the placement of local sensors and assigns linear weights. Through simulations and experiments, we have demonstrated the effectiveness of this local sensor measurement approach. A small number of strategically placed sensors can effectively reconstruct the integral magnetic field with high precision, comparable to conventional measurement techniques. This approach thereby reduces hardware complexity and simplifies the installation of real-time measurement systems. The sensitivity of the method to longitudinal positioning errors of the Hall sensors, especially in high field gradient regions, remains to be evaluated. This methodology presents a scalable, maintainable, and cost-effective alternative to traditional B-Train systems, ensuring reliable integral field monitoring of operational magnets. Its demonstrated effectiveness, validated through its application to the SPS main bending dipoles at the CERN measurement laboratory, which highlights its suitability for modern accelerator facilities.

REFERENCES

- [1] H. Wiedemann, *Particle Accelerator Physics*, Fourth Edition. Springer Nature, Berlin, Germany, 2015. doi:10.1007/978-3-319-18317-6
- [2] N. Sammut, L. Bottura, G. Deferne, and W. V. Delsolaro, “Mathematical formulation to predict the harmonics of the superconducting Large Hadron Collider magnets: III. Pre-cycle ramp rate effects and magnet characterization”, *Phys. Rev. Spec. Top. Accel. Beams*, vol. 12, no. 10, 2009. doi:10.1103/PhysRevSTAB.12.102401
- [3] E. Feldmeier, T. Haberer, M. Galonska, R. Cee, S. Scheloske, and A. Peters, “The First Magnetic Field Control (B-Train) to Optimize the Duty Cycle of a Synchrotron in Clinical Operation”, in *Proc. IPAC’12*, New Orleans, LA, USA, 2012, paper THPPD002, pp. 3503–3505.
- [4] S. Albright *et al.*, “First operational results of new real-time magnetic measurement systems for accelerator control”, in *Proc. IPAC’23*, Venice, Italy, May 2023, pp. 3996–3999. doi:10.18429/JACoW-IPAC2023-THPA024
- [5] M. Buzio, “Fabrication and calibration of search coils”, *arXiv*, 2011. doi:10.48550/arXiv.1104.0803
- [6] M. Amodeo, P. Arpaia, and M. Buzio, “Integrator drift compensation of magnetic flux transducers by feed-forward correction”, *Sensors*, vol. 19, no. 24, 2019. doi:10.3390/s19245455
- [7] C. Grech, M. Buzio, and N. Sammut, “A Magnetic Measurement Model for Real-Time Control of Synchrotrons”, *IEEE Trans. Instrum. Meas.*, vol. 69, no. 2, pp. 393–400, 2020. doi:10.1109/TIM.2019.2904073
- [8] E. Feldmeier, T. Haberer, A. Peters, C. Schoemers, and R. Steiner, “Magnetic Field Correction in Normal Conducting Synchrotrons”, in *Proc. IPAC’10*, Kyoto, Japan, 2010, paper MOPD004, pp. 675–677.
- [9] A. Blondel *et al.*, “Evaluation of the LEP centre-of-mass energy above the W-pair production threshold”, *Eur. Phys. J. C*, vol. 11, no. 4, pp. 573–585, 1999. doi:10.1007/s100529900137
- [10] R. T. Rockafellar, *Convex Analysis*. Princeton University Press, 1970. <https://www.jstor.org/stable/j.ctt14bs1ff>
- [11] U. Hassan and M. S. Anwar, “Reducing noise by repetition: Introduction to signal averaging”, *Eur. J. Phys.*, vol. 31, no. 3, pp. 453–465, 2010. doi:10.1088/0143-0807/31/3/003
- [12] V. di Capua, “Real-time magnetic measurement system for synchrotrons control”, Ph.D. dissertation, Università degli Studi di Napoli Federico II, 2022.
- [13] J. Vella Wallbank, M. Buzio, A. Parrella, C. Petrone, and N. Sammut, “Pulsed-Mode Magnetic Field Measurements with a Single Stretched Wire System”, *Sensors*, vol. 24, no. 14, 2024. doi:10.3390/s24144610